Eur. Phys. J. B **15**, 253–263 (2000)

THE EUROPEAN PHYSICAL JOURNAL B

EDP Sciences

High-pressure synthesis, structural and Raman studies of a two-dimensional polymer crystal of C_{60}

R. Moret[1,a], P. Launois[1], T. Wågberg[2], and B. Sundqvist[2]

[1] Laboratoire de Physique des Solides[b], Bâtiment 510, Université Paris-Sud, 91405 Orsay, France
[2] Department of Experimental Physics, Umeå University, 90187 Umeå, Sweden

Received 8 October 1999

Abstract. Two-dimensional polymerisation of a C_{60} single crystal has been obtained under high-pressure high temperature conditions (700 K - 2 GPa). Crystalline order is preserved but the crystal splits into variants (orientational domains). The analysis of X-ray diffraction and Raman spectroscopy data reveals that the polymer crystal is primarily tetragonal with some admixture of rhombohedral phase. Furthermore, Raman spectroscopy gives evidence for additional C_{60}-C_{60} dimers, which are probably disordered. For the tetragonal phase, it is shown that successive polymer layers are rotated by 90° about the stacking axis, according to the $P4_2/mmc$ space group symmetry. The structure of the rhombohedral phase is also clarified. The role of the interlayer interactions in stabilising the two-dimensional polymer phases of C_{60} is discussed.

PACS. 61.48.+c Fullerenes and fullerene-related materials – 61.50.Ks Crystallographic aspects of phase transformations; pressure effects

1 Introduction

High-pressure polymerisation of C_{60} leads to a variety of new crystalline or amorphous phases that display interesting thermodynamic, structural and physical properties [1]. At temperatures lower than about 700 K and pressure below about 8 GPa, covalent bonding of the fullerene molecules remains essentially linear, thus creating either dimers or 1D molecular chains (Fig. 1). These are formed by covalent linking of neighbouring C_{60} molecules along the $\langle 110 \rangle$ directions of the C_{60} cubic structure. As a result, four-membered rings join the C_{60} molecules and the inter-fullerene C–C bond length is about 1.55 Å corresponding to a short inter-fullerene distance of 9.1–9.2 Å (compared to about 10 Å in pristine C_{60}). The polymer chains are parallel, giving rise to a one-dimensional contraction and they are organised in an orthorhombic lattice [2–9]. Actually, there is evidence that two distinct orthorhombic structures ortho' and ortho, with different lattice parameters, can be prepared in low- and high-pressure regions, respectively [6,8,9] (Fig. 1).

At higher temperature covalent bonding occurs within layers of fullerene molecules and two different types of phases are obtained [2,3,7,10–12]. In the low pressure range (∼ 1 to 4 GPa), C_{60} molecules located in {100} layers from the original cubic structure form covalent bonds, resulting in a tetragonal structure [2,3,7,12]. At higher pressure (∼ 2 to 9 GPa) the polymerisation involves covalent bonding of C_{60} molecules now located in the closed-packed {111} cubic layers. Each molecule is thus trigonaly bound to its six neighbours and the structure is rhombohedral [2,3,7,10–12]. Actually, as indicated above, the low and high pressure regions overlap. While pure

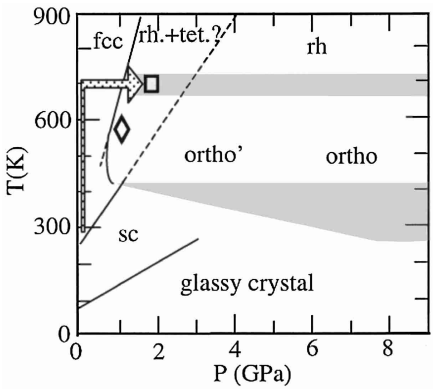

Fig. 1. Diagram illustrating the various C_{60} phases obtained as a function of temperature and pressure in the range 0-900 K and 0-8 GPa (tet: tetragonal phase, rh: rhombohedral phase, ortho′ and ortho: low and high pressure orthorhombic phases, fcc and sc: disordered and ordered C_{60} cubic phases). The dotted lines and shaded areas indicate uncertain or mixed phase. The diamond ◊, refers to the previously reported 1D-polymerisation in a orthorhombic single crystal [5,6]. The arrow points to the conditions of the present pressure-temperature treatment (square □). The diagram is adapted with permission from B. Sundqvist [1b].

[a] e-mail: moret@lps.u-psud.fr
[b] UMR 8502 du CNRS

rhombohedral phase can be produced, the question of the stability of the tetragonal phase is a matter of debate as it is most often mixed with either the 1D orthorhombic or 2D rhombohedral phase [2,3,7,12]. This is indicated by the uncertainty in the phase boundaries of the pressure-temperature diagram (Fig. 1). However, Davydov *et al.* [14–16] recently studied in details the stability of the tetragonal phase using various temperature and pressure treatments and they established that it can be obtained almost pure [15,16].

All C_{60} 1D and 2D polymer phases transform back to the monomeric C_{60} phase upon heating above 300 °C. Early theoretical calculations indicated that the stabilisation energy of the different polymers increases with the number of bonds per C_{60} [17]. In contrast, recent calorimetric measurements by Iwasa *et al.* [18] revealed an opposite behaviour, the 2D polymer phase being less stable than the 1D polymer and dimer phases (though the energy range is very small: ~ 0.01 eV/C atom). Actually, we first point out that the calculations (made at 0 K) do not take into account temperature effects. Furthermore, it has been suggested that the energy required for the deformation of the C_{60} molecules - not considered in the calculations - is in fact larger than the energy gained by the formation of the intermolecular bonds, which may also explain this discrepancy [18]. Okada and Saito [19–21] recently carried out total energy calculations for the 2D polymers within the local-density approximation (LDA). They found that the energy of the rhombohedral phase is very close to that of the fcc monomer phase [19] while the tetragonal phase is more stable [20,21] (0.4059 eV/C_{60} and 0.4286 eV/C_{60} for the tetragonal and rhombohedral phase, respectively).

Another interesting question concerns the nature of the interactions between the polymer chains in the 1D orthorhombic structures and between the polymer layers in the 2D structures. In the orthorhombic structure these interactions determine the relative orientations of the chains. In the 2D tetragonal and rhombohedral polymers the interlayer calculations determine the stacking sequence. The LDA calculations [19–21] show that these interlayer interactions are important and play a role in stabilising both 2D polymer structures. However, they are not the cause of the greater stability of the tetragonal phase, which is attributed to the energy gained *via* the formation of the intermolecular bonds [21].

The formation mechanism of the polymer phases from the C_{60} cubic phase and the transformations between different polymer phases are also intriguing questions which are much debated but still insufficiently documented by experimental results.

Reliable and accurate structural data on these polymers are needed to address the above issues. Powder diffraction studies have provided fundamental structural information on the structure of the C_{60} polymers but the admixture of different phases and/or disorder effects [2,3,10,16] often impedes these studies. Single crystals are obviously difficult to obtain *via* high- pressure high temperature treatments. However, single crystals of the orthorhombic phase were recently synthesised at P = 1-1.2 GPa and T = 550-585 K (see the corresponding mark in Fig. 1) and their study established clearly that the chain ordering corresponds to the Pmnn space group [6].

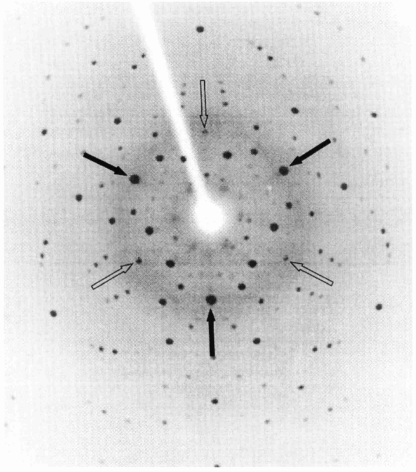

Fig. 2. Laue diffraction pattern (Mo radiation) of the C_{60} crystal prior to the high pressure high temperature treatment. The solid arrows point to a set of 3 reflections from the main crystallite while the open arrows point to equivalent reflections for one of the twin element.

In the present work we report on the synthesis of a single crystal of the 2D polymer, primarily tetragonal but with some admixture of the rhombohedral phase and of disordered C_{60}–C_{60} dimers. The analysis of this single crystal has allowed us to determine the stacking sequence of the C_{60} polymer layers in both tetragonal and rhombohedral phases. The stability of these stacking sequences is discussed on the basis of the intermolecular environments and of the associated interactions.

2 Experimental

The C_{60} crystal used for the high-pressure high-temperature treatment was grown from purified and sublimated C_{60} powder (TechnoCarbo) by controlled sublimation using a two- zone oven (450-500 °C). Its shape is a triangular plate ($\sim 1 \times 1 \times 0.2$ mm). X-ray Laue diffraction patterns were used to detect the presence of twins (stacking faults and associated hexagonal twinning are frequent in face-centred cubic C_{60}). Figure 2 shows a Laue photograph of the C_{60} crystal taken along a $\langle 111 \rangle$ direction; the 3-fold symmetry is visible and the sharp diffraction spots indicate the good quality of the crystal. Note the weak extra spots that correspond to one of the twin elements. Three distinct twin elements were detected, related by reflection in different $\{111\}$ planes. Their volumes are less than 5%, 3% and 2% of the main part of the crystal. We

estimate that the influence of these twins on the polymerisation of the main part of the crystal is small enough to be neglected.

The crystal was compressed in a piston-cylinder device using silicone oil as hydrostatic pressure transmitting medium. It was attached with GE varnish to a glass fibre previously used for the above X-ray Laue characterisation. Heating was accomplished by inserting the sample in a Pyrex glass tube wound with Kanthal wire and electrically insulated by a ceramic coating. Temperature gradients and convection heat losses were minimised by surrounding this oven by spun silica wool. Recent detailed experimental work by Davydov *et al.* [14–16] on a comparison of the temperature-pressure routes leading to the formation of the tetragonal phase showed that the most convenient procedure consists of heating at ambient pressure then pressurising. We followed this procedure and we heated the sample at low pressure to 700 ± 10 K (which is close to the limit of stability of silicone oil) before raising the pressure to 2 GPa. The pressurisation was maintained for ~ 4 hours and the temperature was stable within about 1 K during this treatment. The sample was then quenched to room temperature under pressure, at an initial rate of about 150-200 K/min, before the pressure was released. The high pressure high temperature treatment did not alter significantly the crystal morphology and it was still attached to the glass fibre.

Diffraction patterns have been collected by taking X-ray precession photographs. The CuKα radiation was selected by reflection on a doubly-bent graphite monochromator. Both X-ray films (for a better spatial resolution) and imaging plates (for rapid collections of digitalised data sets) were used to record the patterns. A large collection of precession photographs were taken for the main reciprocal planes relative to the cubic lattice of the parent C_{60} monomer phase. This is justified because of the nearly cubic symmetry produced by the variants, as we will explain below.

The Raman spectrum was measured with a Renishaw 1000 grating spectrometer with a CCD detector. As probing laser we used an argon ion laser (514 nm) with a power density of approximately 1 W/cm^2. The low power density was used to ensure that no damage or further photo-polymerisation was induced to the sample. This was achieved by using a low magnification objective and hence the Raman spectrum represents a mean value of a larger sample area. The resolution of the spectrum is about 2 cm^{-1}.

3 Results and analysis

3.1 X-ray diffraction results

Figures 3a and 4a show typical X-ray precession photographs for the planes $(hhl)_C$ and $(hk0)_C$ (where the index C stands for cubic). These diffraction patterns display distributions of Bragg reflections that exhibit an overall cubic symmetry. They are elongated in the azimuthal direction, corresponding to a large mosaic spread (which depends on the particular reflection, as discussed later). The dramatic increase of the mosaic spread upon polymerisation (compare with the sharp peaks in Fig. 2) may indicate that the polymerisation mechanism involves some inhomogeneous and/or anisotropic processes. The diffraction patterns show similarities with those of the previously studied high pressure C_{60} [5,6] and AC_{60} [22] (A = K, Rb) orthorhombic polymer crystals and cannot be interpreted in terms of the diffraction from a unique single crystal. The observed patterns actually correspond to the combination of orientational domains, so-called variants, as a result of a symmetry lowering. The variants are generated during the formation of the lower symmetry phase (or phases in the case of coexistence of several phases) from the original cubic phase. They are energetically equivalent and they should have, under hydrostatic conditions, equal volumes. The variants are related by the symmetry elements of the cubic structure that are not common to the cubic and low symmetry structures. The contribution of the variants and the superimposition of their diffraction patterns has been taken into account in the analysis, using computer simulations. Note that the contribution of the twin elements present in the parent C_{60} crystal has been neglected in the course of the X-ray analysis (the largest twin element being 5% of the main crystal part).

In a first stage we focus our analysis on the geometrical aspects of the diffraction patterns to derive the characteristics of the lattice, without considering the intensity (and possible extinction conditions) of the reflections. This enables us to determine the unit cell and also the orientation of the variants relative to the cubic lattice. The mosaic spread was evaluated by fitting to the experimental patterns. Considering that the high pressure high temperature polymerisation conditions were chosen so as to lead to the tetragonal polymer phase we first analyse the data in terms of a tetragonal lattice. A satisfactory (but partial, see below) agreement with the observed patterns can be obtained with $a_T = 9.02 \pm 0.04$ Å and $c_T = 14.93 \pm 0.05$ Å. Furthermore, it is found that the directions of the tetragonal ($\mathbf{a}_T$, $\mathbf{b}_T$, $\mathbf{c}_T$) and cubic ($\mathbf{a}_C$, $\mathbf{b}_C$, $\mathbf{c}_C$) axes are related as follows:

$$\mathbf{a}_T = \frac{(\mathbf{a}_C + \mathbf{b}_C)}{2}$$

$$\mathbf{b}_T = \frac{(-\mathbf{a}_C + \mathbf{b}_C)}{2}$$

$$\mathbf{c}_T = \mathbf{c}_C.$$

These relations imply that, upon the formation of the tetragonal phase, the directions of polymerisation of the C_{60} molecules remain aligned along the original $\langle 110 \rangle_C$ directions. Thus, the $(100)_C$ layers of C_{60} molecules transform into the $(001)_T$ layers of 2D-polymerized C_{60} and there is no disorientation of the lattice with respect to the cubic one. It is at variance with the case of the orthorhombic 1D polymers, where the $\langle 110 \rangle_C$ chains rotate as a result of a polymerisation mechanism which preserves the orientation of a $(111)_C$ plane [6]. In the 1D case, twelve

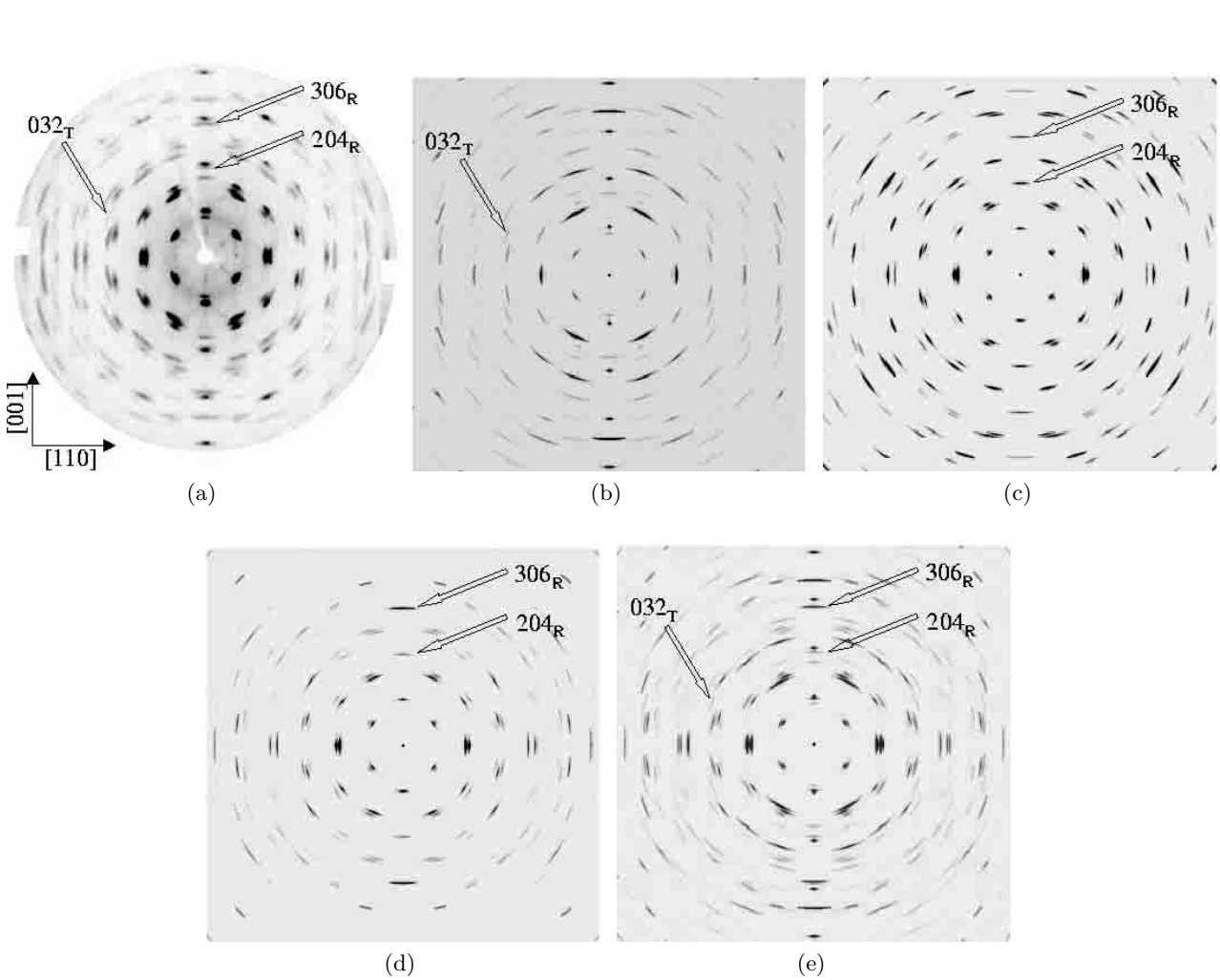

Fig. 3. (a) $(hhl)_C$ diffraction pattern (CuKα precession photograph) of the polymer crystal. Groups of reflections, sometimes overlapping, are the signature of the complex structure of the crystal (tetragonal and rhombohedral phases + variants). Note that the reflections exhibit different mosaic spreads. Some characteristic reflections mentioned in the text are labelled. (b) Calculated pattern for the 3 tetragonal variants. (c) Calculated pattern for the 4 rhombohedral variants (structural model I). (d) Calculated pattern for the 4 rhombohedral variants (structural model II). (e) Calculated pattern resulting from the combination of the tetragonal and rhombohedral (structural model II) variants.

distinct variants had to be taken into account (only one mirror plane and the centrosymmetry were common to the cubic and orthorhombic point groups) while in the present case the tetragonal mirror planes originate from cubic mirror planes so that only three variants are generated. These variants are related by the cubic 3-fold axes. The superimposition of their diffraction patterns leads to the simulated $(hhl)_C$ pattern shown in Figure 3b.

The cell parameters can be compared with those deduced from powder experiments by Núñez-Regueiro *et al.* [2] (9.09 Å and 14.95 Å at 973 K and 4 GPa) and by Davydov *et al.* [7] (9.073 Å and 15.111 Å at 873 K and 2.5 GPa). The present single crystal values, and in particular the a_T parameter (corresponding to covalent bonding along the a and b directions) are found to be shorter than those reported previously. This is not currently understood given that the present low temperature-pressure conditions would rather be in favour of a larger unit cell volume.

A comparison of the experimental and calculated diffraction patterns reveals that some of the observed peaks are not accounted for by the sole contributions of the tetragonal variants. We therefore consider the possibility of a coexistence of the tetragonal phase with other phases (including their respective variants). The patterns show no evidence for the presence of the orthorhombic phase while reflections from the rhombohedral phase can be identified unambiguously. The rhombohedral variants originate from polymerisation which takes place within one of the four $(111)_C$ cubic layers of C_{60} molecules. By fitting the calculated patterns to the observed ones we find that its orientation is in fact unchanged from that of the original $(111)_C$ cubic. Four rhombohedral variants are thus generated, corresponding to the four cubic 3-fold

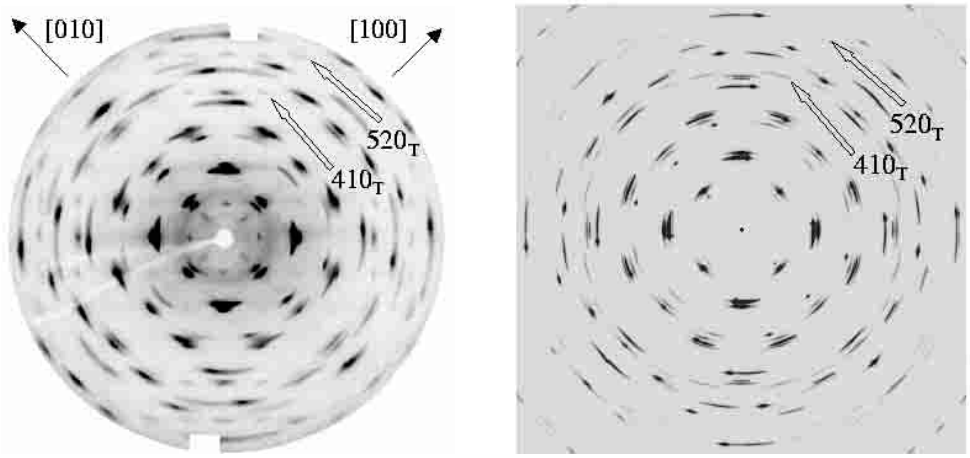

(a) (b)

Fig. 4. (a) $(hk0)_C$ diffraction pattern (CuKα precession photograph) of the polymer crystal. Note that the four-fold symmetry is broken due to non-equivalent tetragonal variants. Reflections $(410)_T$ and $(520)_T$, *i.e.* with $h + k + l$ odd, are visible. (b) Calculated tetragonal + rhombohedral (model II) patterns.

axes that become the stacking directions of the trigonally polymerised layers.

The relation between the directions of the rhombohedral and cubic axes is:

$$\mathbf{a}_R = \frac{(\mathbf{a}_C - \mathbf{b}_C)}{2}$$
$$\mathbf{b}_R = \frac{(\mathbf{b}_C - \mathbf{c}_C)}{2}$$
$$\mathbf{c}_R = \mathbf{a}_C + \mathbf{b}_C + \mathbf{c}_C.$$

A satisfactory agreement with the observed patterns is obtained using the unit cell parameters previously determined by Núñez-Regueiro *et al.* [2] (9.19 Å and 24.5 Å at 700 K and 4 GPa) or Iwasa *et al.* [10] (9.22 Å and 24.6 Å at 500-800 K and 5 GPa) (due to the complexity and relatively poor resolution of the diffraction patterns both sets of parameters provide equally satisfactory fits to the data).

We now examine the reflection intensities to gain some information on the stacking sequences of the tetragonal and rhombohedral phases. Structural models for the tetragonal and rhombohedral phases of C_{60} have been proposed on the basis of pioneering experimental and theoretical studies [2,10,11,17]. In the tetragonal phase, successive layers of covalently bonded C_{60} molecules (originating from $(100)_C$ layers in the parent cubic C_{60} structure, Fig. 5a) were found to be stacked along $\mathbf{c}_T$ and shifted by $(\mathbf{a}_T + \mathbf{b}_T + \mathbf{c}_T)/2$, corresponding to the Immm space group symmetry, as shown in Figure 5b. Note that this structure is actually orthorhombic and not tetragonal, which could give rise to a small distortion in the form of different a_T and b_T parameters. In the rhombohedral phase, Núñez-Regueiro *et al.* [2] proposed that the trigonal layers of C_{60} molecules (originating from $(111)_C$ layers in the parent cubic C_{60} structure) are stacked in a close-packed arrangement of the type ABCABC in the space group R $\bar{3}$ m (where A, B and C denote C_{60} molecules at 0,0; 2/3, 1/3; 1/3, 2/3 within their respective layer).

These structures were recently reconsidered by Davydov *et al.* [13–16], using both powder X-ray diffraction and lattice energy minimisation methods. A different type of stacking was proposed for the tetragonal structure - where the successive 2D polymer layers are rotated by 90° - corresponding to the (truly tetragonal) space group $P4_2/mmc$ (Fig. 5c). This stacking was found to be ~ 4 kJ/mol more stable than the Immm one.

For the rhombohedral R $\bar{3}$ m structure it was pointed out [13], interestingly enough, that the ABCABC and ACBACB stacking sequences of polymerised C_{60} layers are not equivalent, due to the fact that the symmetry of the individual layers is actually trigonal and not hexagonal (in contrast to the case of rhombohedral or face-centred cubic packing of atoms). An equivalent description of the difference between these two structures consists in introducing a 60-degree rotation of the C_{60} molecules around the 3-fold stacking axis while keeping the same stacking sequence, for instance ABCABC (Figs. 5d,e). It was found that rotating the molecules in model I (Fig. 5d) by 60° leads to a more stable structure (by ~ 20 kJ/mol, model II, Fig. 5e). Moreover, Davydov *et al.* [13] proposed that an hypothetical combination of model I and II, where the two types of layers alternate along **c**, would give an even slightly more favourable structure (model III).

It is somewhat difficult to distinguish between the different structural models described above (for both tetragonal and rhombohedral phases) because they produce relatively similar diffraction data. This is due to the nearly spherical symmetry and the large number of atoms in the C_{60} molecule (C_{60} can often be approximated to a homogeneous spherical shell). It follows that diffraction effects are not very sensitive to the orientation of the C_{60} molecules, while the difference between the structural models is mainly orientational in nature. At present,

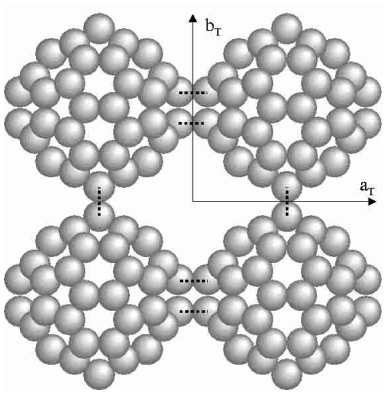

(a)

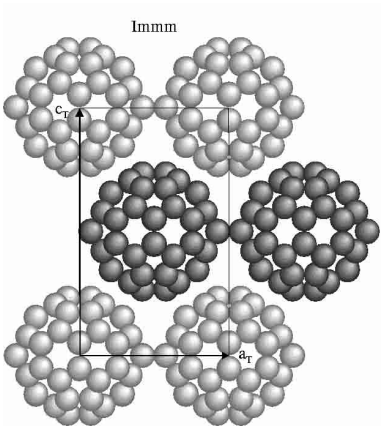

(b)

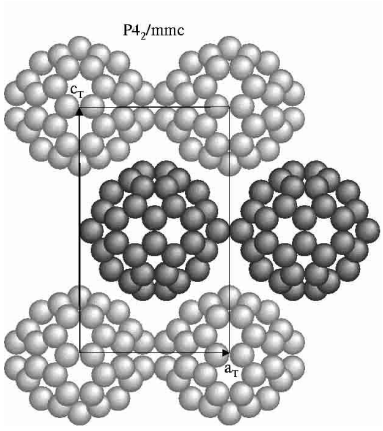

(c)

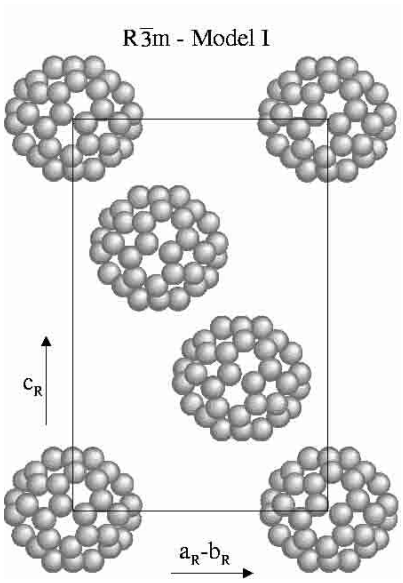

(d)

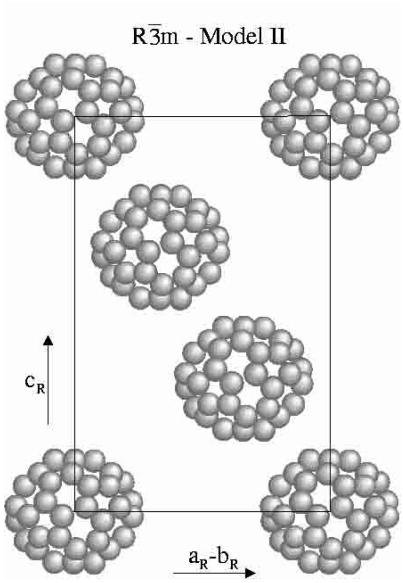

(e)

Fig. 5. Structures of the 2D polymers of C_{60}: (a) Layer of C_{60} molecules linked by [2 + 2] cycloaddition in the tetragonal polymer. Dotted lines represent covalent bonds. (b) Immm model for the stacking of the C_{60} layers in the tetragonal polymer (the darker molecules are shifted by (1/2, 1/2, 1/2) with respect to the lighter ones). (c) $P4_2/mmc$ model for the stacking of the C_{60} layers in the tetragonal polymer (same as above). (d) View of the rhombohedral structure in the (1 $\bar{1}$ 0) plane, according to model I. (e) View of the rhombohedral structure in the (1 $\bar{1}$ 0) plane, according to model II. Notice the different orientation of the molecules as compared to (d). It corresponds to a 60° rotation around **c**.

the sensitivity of the available powder diffraction data [2,10,13–16] to these orientational effects is not sufficient to distinguish between the above models and single crystals studies are expected to provide more detailed information (as it was shown for the case of the orthorhombic polymer [6]).

For the tetragonal structure the distinction between Immm and $P4_2/mmc$ can be made on the basis of the existence or absence of reflections with $h+k+l$ odd, which characterise a primitive or body-centred lattice, respectively. A detailed analysis of Figures 3a and 4a together with the calculated patterns of Figures 3b and 4b reveals the presence of weak "$h+k+l$ odd" reflections such as $(032)_T$, $(410)_T$, $(520)_T$ (as marked in the figures). This observation rules out a body-centred structure and validates the $P4_2/mmc$ structural model (Fig. 5c). The comparison of the experimental and simulated patterns also reveals that (i) the 3 variants do not have equal contributions (this is responsible for the lack of 4-fold symmetry in Fig. 4a, for instance), (ii) the azimuthal broadening of the reflections depends on the variant. This shows that the variants do not have the same volume and mosaic spread. We have obtained a satisfactory semi-quantitative agreement with the data assuming that one of the variants has a volume that is 5 times as large as that of the others and a mosaic spread that is narrower (0.9° as compared to 4.5°, HWHM). The unexpected non-equivalence of the variants may be due to slightly non-hydrostatic pressure conditions or/and to extended defects that introduce some anisotropy. The fact that the crystal was glued to a glass fibre may be partly responsible for the non-hydrostatic conditions. The intensity calculation was performed assuming that the distortion of the C_{60} molecule due to bonding is locally – *i.e.* close to the bonds – the same as in the 1D polymers. In view of the complexity of the crystal (variants, mosaic spread) it is not possible to refine the parameters of this distortion or to obtain more quantitative information.

We now turn to the structure of the rhombohedral phase. Let us note that we have evaluated the relative weights of the tetragonal and rhombohedral components. It turns out that the volume occupied by the 4 variants of the rhombohedral phase is smaller than that of the tetragonal one by a factor $\sim$ 3–4. Furthermore, the mosaic spread of the rhombohedral variants is on the order of 3° (HWHM).

While all three models for the rhombohedral structure correspond to R $\bar{3}$ m and thus cannot be determined on the basis of different extinction conditions, model III is associated with a doubling of the lattice parameter along c and it can be ruled out because the corresponding supplementary reflections have not been detected. It is more difficult to distinguish between models I and II as they differ by relatively small intensity variations. The quality of the crystal precludes a detailed intensity refinement and we have restricted ourselves to a comparison of the relative intensities, I_{hkl}, of a few reflections with those calculated for the two models. This comparison indicates that model II provides a better fit to the available data than model I. Note for example that $I_{306} > I_{204}$ (Fig. 3a), which is verified for model II (Fig. 3d) but not for model I, where $I_{306} < I_{204}$ (Fig. 3c). Although a more detailed and accurate analysis will be useful to ascertain this finding our present results indicate that the structure taken up by 2D rhombohedral C_{60} is represented by model II (Fig. 5e).

In summary, the analysis of the single crystal diffraction data shows that the crystal consists primarily of variants of the tetragonal phase and that the polymerisation mechanism involves no disorientation of the lattice with respect to the parent cubic C_{60} structure. The stacking of the polymerised C_{60} layers corresponds to the $P4_2/mmc$ space group (and not the orthorhombic Immm). The crystal also contains a fraction (3-4 times as small) of rhombohedral phase and a preliminary analysis indicates that its structure is different from that previously proposed [2] (specifically the molecules are further rotated by 60° about the stacking axis) but it is in agreement with recent calculations of the relative stability of the stacking sequences [13].

3.2 Raman scattering results

The Raman spectrum of pristine C_{60} contains 10 active $A_g + H_g$ modes, consistent with the I_h symmetry of the C_{60} molecule. The frequencies of these are shown in Figure 6 as vertical lines at the bottom of the figure. Figure 6 also shows the Raman spectrum of our polymerised sample. When the molecules in the sample connect and form a tetragonally polymerised structure, the molecular symmetry is expected to decrease from the I_h symmetry to the D_{2h} symmetry. This lowering of the symmetry leads to a number of new Raman active modes together with a split of the five-fold degenerated H_g modes. This splitting is especially clear for the $H_g(3)$ and $H_g(4)$ modes in our Raman spectrum, originally at 711 cm^{-1} and 775 cm^{-1}. For some modes this splitting is not as evident, for example the $H_g(2)$ mode at 430 cm^{-1}. The reason for this is that the new components are much less intense than the mode at 430 cm^{-1} due to a resonance enhancement of this particular mode by the probing Ar laser [23]. The new modes which appear are in most cases former optically silent modes that now are visible due to the new symmetry point group. Examples of this are seen at 535 cm^{-1} and 1208 cm^{-1}, probably originating from the F_{2g} (1) mode and the odd parity F_{1u} (3) mode. Another very strong new mode located around 950 cm^{-1} is characteristic for [2+2] cycloadducted phases, corresponding to the frequency of the cyclobutane bond vibrations in the intermolecular four- membered ring [24]. Even though the Raman spectra of the different polymerised C_{60} phases are very complex and rather similar it is possible to find characteristic modes for different phases. One such fingerprint for the tetragonal phase is the mode pattern between 600 cm^{-1} and 800 cm^{-1}, especially the double peak at 742 cm^{-1} and 748 cm^{-1}. In addition to these peaks the shift of the pentagonal pinch mode at 1469 cm^{-1} to lower frequencies has proven to be a very powerful probe of the state of the polymerisation. For the tetragonal phase

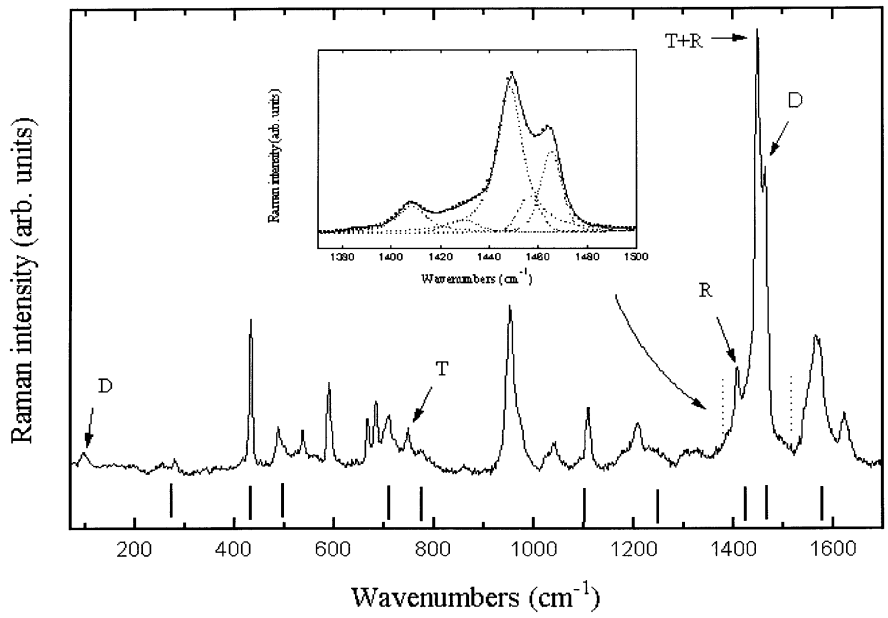

Fig. 6. Raman spectrum of the polymer crystal between 70 cm^{-1} and 1700 cm^{-1}. Vertical ticks show the position of the modes for pristine C_{60}. The inset shows fitted peaks (dotted lines), in the region (1380 and 1520 cm^{-1}) indicated by vertical dotted lines, of the $A_g(2)$ pentagonal pinch mode.

this mode shifts to $\approx$ 1448 cm^{-1}. This is in good agreement with calculations made by Porezag *et al.* who showed that the shift of the $A_g(2)$ mode is linearly dependent on the number of covalent bonds on the molecule [25]. The mode at 1448 cm^{-1} has however also been reported for pure rhombohedral samples and could be characteristic for both phases [12]. Most of the characteristic peaks mentioned here for the tetragonal phase are in excellent agreement with previous reports by Davydov *et al.* [14], who treated polycrystalline C_{60} at 2.2 GPa and 873 K. The similarity also includes the peak at 1408 cm^{-1} which is discussed below. Some discrepancies can however also be mentioned, for example the region around the former $H_g(3)$ mode where the mode at 711 cm^{-1} is much stronger in the Raman spectrum for our sample than in that of Davydov *et al.* [14]. Other polymerised phases also have characteristic shifts of the pentagonal pinch mode. It has been shown that the dimer phase (one bond per molecule) is characterised by a shift to $\approx$ 1464 cm^{-1} [26–29] and the phase containing linear polymeric chains (two bonds per molecule) by a shift to $\approx$ 1459 cm^{-1} [27,30,31]. To resolve the different peaks and their intensities in the region of the pentagonal pinch mode we have used a peak-fitting program to fit peaks between 1380 cm^{-1} and 1520 cm^{-1}. The result of this fit is shown as an inset in Figure 6. The dominating peak is located at 1448 cm^{-1} and amounts to 57.3% of the total peak area, not including the very weak mode at 1428 cm^{-1} which is probably the former $H_g(7)$ mode in this area. The second most intense peak is found at 1465 cm^{-1}, making up 21.2% of the total peak area. As mentioned, this mode is characteristic for dimers but it could also be some other characteristic mode for the tetragonally polymerised phase. However, the dimer phase is not only characterised by the 1464 cm^{-1} mode but also by an intermolecular mode at 97 cm^{-1} [26–29], representing the vibration of two molecules connected by the 2+2 cycloaddition. Looking at the Raman spectrum in Figure 6, a distinct mode can be found at 97 cm^{-1}, giving very strong support that our crystal also contains a significant fraction of dimers. Unfortunately the volume fraction of dimers is very hard to determine from a Raman spectrum since the Raman cross sections for the $A_g(2)$ modes of the different phases are not known. Looking at the other peaks in the fitted region a very weak mode ($\approx$ 8%) can be found at 1457 cm^{-1}, probably indicating a very small fraction of the orthorhombic phase. In addition a peak at 1408 cm^{-1} can be clearly seen in the spectrum (12.6%). This mode has been reported to be a fingerprint for the rhombohedral phase [29] and the Raman spectrum therefore supports our X-ray results, discussed above, which also indicate a small fraction of the rhombohedral phase.

To summarise, our Raman results show that a dominant part of our crystal consists of tetragonally polymerised C_{60}. In addition, we find a peak at 1408 cm^{-1} indicating a minor fraction of rhombohedral phase. Together with these phases we find strong evidence that it also contains a fraction of dimers, represented by peaks at 1464 cm^{-1} and 97 cm^{-1}. The relative fractions of the different phases is difficult to determine from the Raman data.

4 Discussion

Our results show that it is possible to obtain 2D fullerene polymers by treating C_{60} single crystals under high-pressure high-temperature conditions and without destroying the crystal. Following recent results [14,16]

the conditions adopted here (2 GPa-700 K; heating the sample before establishing the pressure) were aimed at obtaining pure tetragonal phase. However, although our polymerised crystal contains a major fraction of this phase, significant amounts of rhombohedral phase and of C_{60}–C_{60} dimers are identified. The presence of the rhombohedral phase is established by both X-ray diffraction and Raman spectroscopy but the situation is different for the dimers. Whereas Raman spectroscopy strongly advocates the presence of C_{60}–C_{60} dimers, the analysis of the diffraction patterns reveals no signature from the dimers. This may be due to the small fraction of dimers in the crystal but also to the fact that they may be in a disperse and disordered state. Disordered distributions of the dimers would produce some specific but relatively weak diffuse scattering intensity which may not be visible on the precession photographs used in this study. Further work, employing X-ray diffuse scattering experimental techniques, is in progress to characterise the state of order of the dimers.

The observation of a mixture of phases in our polymerised crystal would not be inconsistent with the pressure-temperature diagram of Figure 1, as the pressure and temperature used here correspond to an ill-defined region. However, recent extensive investigations performed on powders [14–16] showed that (i) a treatment at 2.2 GPa and 873 K, using the same procedure as followed here (heating first then pressurising) leads to pure tetragonal phase after 1000 s [14] (ii) at lower pressure 1.5 GPa and in the range 723-900 K the tetragonal phase should be the more stable, although some admixture of orthorhombic and dimer phases were observed for short reaction times [16]. The conditions of the present study (2 GPa-700 K) are not strictly covered by the above investigations but, from the tentative $P-T$ diagram of Davydov *et al.* [14–16], pure tetragonal phase was expected. The mixture of phases observed in our crystal and in particular the presence of a significant amount of rhombohedral phase suggest that the stability regions of these phases are still unclear. Other remarks can be made in this respect. It is possible that the processes involved during the polymerisation depend on the presence of defects or on size effects, which can be different for powder and single crystal samples. Therefore, the same treatment applied to powders and single crystals may produce different results. It is also worth noting that the single crystal pressure treatment may not have been fully isotropic. In particular, the crystal was not completely free in the silicon oil used as a pressure medium because the glass fibre it was glued to could have produced anisotropic constraints.

We now discuss the stacking of the polymer layers in both tetragonal and rhombohedral phases. The $P4_2/mmc$ tetragonal stacking model proposed here is characterised by a 90°-rotation of successive C_{60} layers. It is more symmetric than the original orthorhombic Immm model [2,6] which would allow a slight difference between the a_T and b_T parameters. An evaluation of the stability of these two types of stacking was done recently by Davydov *et al.* using optimal packing calculations [13,16]. These calculations were based on intermolecular potentials built for solid C_{60} from Lennard-Jones and electrostatic interactions by Lu *et al.* [32]. We recall that, in the case of pristine C_{60}, the various intermolecular potentials have been evaluated using the diffuse scattering produced by the orientational local order as a testing ground, which showed that none of potentials currently proposed is fully satisfactory [33]. The potential proposed by Lu *et al.* [32] was designed to account for the C_{60} low temperature $Pa\bar{3}$ phase [34] while its ability to reproduce the observed modulations of the room temperature diffuse scattering intensity was found to be limited [33]. Moreover, one should keep in mind that the polymer phases are formed at high temperature while the calculations are performed to obtain the energy at 0 K and not the free energy. Within these restrictions on the validity of the current intermolecular potentials and on the role of temperature it is still very interesting that the $P4_2/mmc$ was predicted to be more stable by $\sim$ 4 kJ/mol [13,16], in agreement with our experimental findings. The total energy LDA calculations of the tetragonal polymer phase by Okada and Saito [21], found that the tetragonal layer is slightly distorted (a_T smaller than b_T, for instance), which is not compatible with the Immm structure and supports either the $P4_2/mmc$ stacking sequence or the existence of stacking disorder. These studies concluded that the interlayer interactions are sizeable but they were made for the Immm case and did not compare the stability of the Immm and $P4_2/mmc$ structures. Along these lines, it is also worth to mention that a very recent calculation, using the same procedure, of the effect of uniaxial pressure on the Immm structure predicted the formation of a three-dimensional metallic polymer with a relatively large density of states at the Fermi level [36]. It would thus be interesting to examine whether a comparable three-dimensional polymerisation can be stabilised for the $P4_2/mmc$ structure.

As the stability of different stackings is related to the intermolecular van der Waals and Coulomb forces between near-neighbour C_{60} molecules from successive layers, it is useful to visualise the environment of these molecules. Figure 7 shows 2 molecules - represented by the grey and black bonding frames - facing each other in the case of the Immm and $P4_2/mmc$ stackings. For other phases [22,35] such representations have helped to distinguish between different structural models. However, in this particular case, an examination of Figures 7a,b reveals that the two configurations are quite similar and it is difficult to understand the origin of the stabilisation of the $P4_2/mmc$ stacking. The small energy difference calculated by Davydov and coworkers [13,16] is thus probably due to a subtle combination of interaction energies, which cannot be understood on simple grounds.

In the case of the rhombohedral structure, the stacking we put forward here differs from that originally proposed by Núñez-Regueiro *et al.* [2] in that the C_{60} are rotated by 60° about **c**, as pointed out by Davydov *et al.* [13] (model II, Fig. 5e). Figure 8 shows the environment of two near-neighbour C_{60} molecules for

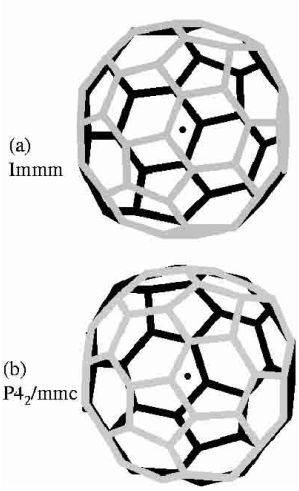

Fig. 7. Near-neighbour molecular environments viewed along the [111] directions for the Immm (a) and P4$_2$/mmc (b) tetragonal models. The black C–C bond frame of the more distant molecule is viewed through a portion of the grey C–C bond frame of the nearer one. The central dot represents the projection of the centres of the two molecules.

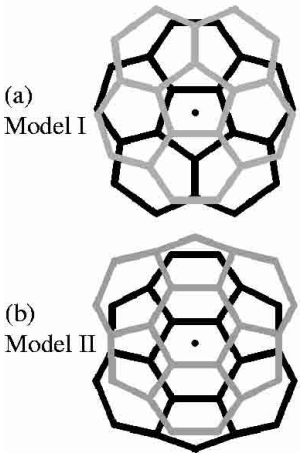

Fig. 8. Near-neighbour molecular environments viewed along the [1$\bar{1}\bar{1}$] directions for the rhombohedral models I (a) and II (b). The black C–C bond frame of the more distant molecule is viewed through a portion of the grey C–C bond frame of the nearer one. The central dot represents the projection of the centres of the two molecules.

models I (Fig. 8a) and II (Fig. 8b) (in a similar way as in Fig. 7 for the tetragonal structure). Significant differences can be identified between the two models. In model I, pentagons almost face each other along the near-neighbour direction (Fig. 8a) while, for model II, C = C bonds approximately face hexagons on the neighbouring molecule. The electron density on a C_{60} molecule is such that the pentagons and to a lesser extent the hexagon centres are electron-poor regions while the double bonds are electron-rich (which provides a simple way to understand the orientational ordering of the C_{60} molecules in the low-temperature Pa$\bar{3}$ phase of C_{60} [35]). Assuming that this electronic distribution is not perturbed too strongly in the polymer, at least for the regions of the molecules which are not directly affected by the covalent bonding, we can propose a simple electrostatic scheme to differentiate the two models. Model II, where electron-rich double bonds are approximately aligned over the electron-deficient hexagons, appears to be more favourable than model I, where electron-poor pentagons are almost facing. Finally, we point out that our results are in agreement with the predictions of Davydov *et al.* who calculated (using the same type of intermolecular potential as discussed above for the tetragonal structures) a relatively large energy difference (20 kJ/mol) between the two structural models, in favour of model II [13,16]. The total energy LDA calculations of the rhombohedral phase by Okada and Saito [19] did not consider other types of stacking than that of model I.

We now comment on the possible mechanism of polymerisation for the present phases produced by pressurising the sample after the temperature had been raised to 700 K. We recall that, at room temperature, in the fcc phase, the C_{60} molecules rotate rapidly but their orientations exhibit weak and complex correlations with several, almost degenerate, configurations [33]. Polymerisation through [2 + 2] cycloaddition requires that double bonds on neighbouring molecules face each other, which can occur due to the rotational motion. On the other hand we point out that in both tetragonal P4$_2$/mmc (Fig. 7b) and rhombohedral R $\bar{3}$ m structures (Fig. 8b), near-neighbour molecules that belong to successive polymer layers are close to a "hexagon facing double-bond" configuration. Such a configuration (together with the "pentagon facing double-bond" which stabilises the low-temperature simple cubic phase [35]) is among the preferred configurations at room temperature and ambient pressure. Furthermore, pressure is known to stabilise the "hexagon facing double-bond" configuration [1]. These observations lead us to suggest that the "hexagon facing double-bond" configurations present in fcc C_{60} play a role in the formation of the tetragonal and rhombohedral phases. This is however tentative because the intermolecular correlations are certainly quite weak at 700 K. Using a different approach, Davydov *et al.* [9,14] propose a two-stage model for the formation of the polymer phases and they suggest that there exists an intermediate precursor state for each of the polymers, where the C_{60} molecules would be almost well oriented for cycloaddition. This state would correspond to a local potential energy minimum and its structure would resemble that of the final polymer phase. For instance, they propose a quasi-tetragonal structure as a precursor towards the tetragonal phase. More details along these lines are much awaited. Finally we note that the observation of dimers in the crystal supports the view that dimerisation may be a preliminary stage towards polymerisation. If this is the case, the fact that all the dimers have not transformed into 2D polymers may be due to slow kinetic processes. Slow polymerisation evolutions have been observed under various conditions [16]. Furthermore, as already discussed above, it is possible that single crystals behave differently from powders, especially when kinetics is considered. Obviously, much more information needs to be gathered in order to understand

the complex mechanisms involved in the formation of the C_{60} polymers.

It would be interesting to try polymerise single crystals in different conditions and using various routes in the $P-T$ diagram, as shown by the following examples. The transformation from the 1D orthorhombic polymers to the 2D polymers is quite intriguing as it implies a reorientation of the 1D chains about their axes in order to form either tetragonal or trigonal layers of polymerised C_{60} molecules. The conversion of the rhombohedral to the tetragonal phase, observed by Davydov *et al.* [14], is also challenging but difficult to achieve in single crystals. We also mention that a study of the formation of the dimers from monomeric C_{60} and the description of the local order of the dimers is currently underway.

To conclude we emphasise the value of studying the orientational ordering properties of the polymer phases (local order for the dimers, chain orientation for the 1D polymers, layer stacking for the 2D polymers) because it is most often a prerequisite to the understanding of their properties.

The authors would like to thank V. Agafonov for fruitful discussions and for communicating his results prior to publication. A. Soldatov and E. Sandré are thanked for helpful discussions. R.M. and P.L. acknowledge support by the C.N.R.S. under the French-Swedish international cooperation. T.W. and B.S. acknowledge financial support by the Swedish Research Councils for Natural Science (NFR) and Engineering Science (TFR).

References

1. For recent reviews, see for instance (a) V.D. Blank, S.G. Buga, G.A. Dubitsky, N.R. Serebryanaya, M. Yu. Popov, B. Sundqvist, Carbon **36**, 319 (1998); (b) B. Sundqvist, Adv. Phys. **48**, 1 (1999).
2. M. Núñez-Regueiro, L. Marques, J.-L. Hodeau, O. Béthoux, M. Perroux, Phys. Rev. Lett. **74**, 278 (1995).
3. L. Marques, J.-L. Hodeau, M. Núñez-Regueiro, M. Perroux, Phys. Rev. B **54**, R12633 (1996).
4. P.-A. Persson, U. Edlund, P. Jacobsson, D. Johnels, A. Soldatov, B. Sundqvist, Chem. Phys. Lett. **258**, 540 (1996).
5. B. Sundqvist, O. Andersson, U. Edlund, Å Fransson, A. Inaba, P. Jacobsson, D. Johnels, P. Launois, C. Meingast, R. Moret, T. Moritz, P.-A. Persson, A. Soldatov, T. Wågberg, in *Fullerenes: Recent Advances in the Chemistry and Physics of Fullerenes and Related Materials*, vol. 3, edited by K.M. Kadish, R.S. Ruoff (The Electrochemical Society Proceedings, ECS, Pennington, NJ, 1996), p. 1014.
6. R. Moret, P. Launois, P.-A. Persson, B. Sundqvist, Europhys. Lett. 40, 55 (1997); P. Launois, R. Moret, P.-A. Persson, B. Sundqvist, in *Molecular Nanostructures*, edited by H. Kuzmany, J. Fink, M. Mehring, S. Roth (World Scientific, Singapore, 1998), pp. 348-352.
7. V.A. Davydov, L.S. Kashevarova, A.V. Rakhmanina, V. Agafonov, R. Ceolin, H. Szwarc, Carbon **35**, 735 (1997).
8. V. Agafonov, V.A. Davydov, L.S. Kashevarova, A.V. Rakhmanina, A. Kahn-Harari, P. Dubois, R. Céolin, H. Szwarc, Chem. Phys. Lett. **267**, 193 (1997).
9. V.A. Davydov, L.S. Kashevarova, A.V. Rakhmanina, A.V. Dzyabchenko, V. Agafonov, P. Dubois, R. Ceolin, H. Szwarc, JETP Lett. **66**, 120 (1997).
10. Y. Iwasa, T. Arima, R.M. Fleming, T. Siegrist, O. Zhou, R.C. Haddon, L.J. Rothberg, K.B. Lyons, H.L. Carter Jr., A.F. Hebard, R. Tycko, G. Dabbagh, J.J. Krajewski, G.A. Thomas, T. Yagi, Science **264**, 1570 (1994).
11. G. Oszlanyi, L. Forro, Solid State Com. **93**, 265 (1995).
12. A.M. Rao, P.C. Eklund, J.-L. Hodeau, L. Marques, M. Núñez-Regueiro, Phys. Rev. B **55**, 4766 (1997).
13. V.A. Davydov, V. Agafonov, A.V. Dzyabchenko, R. Ceolin, H. Szwarc, J. Solid State Chem. **141**, 164 (1998).
14. V.A. Davydov, L.S. Kashevarova, A.V. Rakhmanina, V. Agafonov, H. Allouchi, R. Ceolin, A.V. Dzyabchenko, V.M. Senyavin, H. Szwarc, Phys. Rev. B **58**, 14786 (1998).
15. V.A. Davydov, V. Agafonov, H. Allouchi, R. Ceolin, A.V. Dzyabchenko, H. Szwarc, Synth. Metals **103**, 2415 (1999).
16. V.A. Davydov, L.S. Kashevarova, A.V. Rakhmanina, V. Agafonov, H. Allouchi, R. Ceolin, A.V. Dzyabchenko, V.M. Senyavin, H. Szwarc, T. Tanaka, K. Komatsu, J. Phys. Chem. B **103**, 1800 (1999).
17. C.H. Xu, G. Scuseria, Phys. Rev. Lett. **74**, 274 (1995).
18. Y Iwasa, K. Tanoue, T. Mitani, T. Yagi, Phys. Rev. B **58**, 16374 (1998).
19. S. Okada, S. Saito, Phys. Rev. B **55**, 4039 (1997).
20. S. Saito, S. Okada, in *Electronic Properties of Novel Materials, XII International Winterschool*, edited by H. Kuzmany *et al.* (The American Institute of Physics, 1998), p. 198.
21. S. Okada, S. Saito, Phys. Rev. B **59**, 1930 (1999).
22. P. Launois, R. Moret, J. Hone, A. Zettl, Phys. Rev. Lett. **81**, 4420 (1998).
23. T. Wågberg, A. Soldatov, B. Sundqvist (unpublished).
24. F.A. Miller, R.J. Capwell, R.C. Lord, D.G. Rea, Spectrochim. Acta A **28**, 603 (1972).
25. D. Porezag, M.R. Pederson, T. Frauenheim, T. Köhler, Phys. Rev. B **52**, 14693 (1995).
26. S. Lebedkin, A. Gromov, S. Giesa, R. Gleiter, B. Renker, H. Rietschel, W. Krätschmer, Chem. Phys. Lett. **285**, 210 (1998).
27. B. Burger, J. Winter, H. Kuzmany, Z. Phys. B **101**, 227 (1996).
28. T. Wågberg, P.-A. Persson, B. Sundqvist, P. Jacobsson, in *Fullerenes: Recent Advances in the Chemistry and Physics of Fullerenes*, edited by K.M. Kadish, R.S. Ruoff (Electrochemical Society, Pennington, 1997), vol. 5, p. 674.
29. T. Wågberg, P.-A. Persson, B. Sundqvist, J. Phys. Chem. Solids (in press).
30. P.C. Eklund, P. Zhou, K-A. Wang, G. Dresselhaus, M.S. Dresselhaus, J. Phys. Chem. Solids **53**, 1391 (1992).
31. T. Wågberg, P. Jacobsson, B. Sundqvist, Phys. Rev. B **60**, 4535 (1999).
32. J.P. Lu, X.P. Li, R. Martin, Phys. Rev. Lett. **68**, 1551 (1992).
33. P. Launois, S. Ravy, R. Moret, Phys. Rev. B **55**, 2651 (1997); **56**, 7019 (1997); P. Launois, S. Ravy, R. Moret, Int. J. Mod. Phys. B **13**, 253 (1999).
34. A.V. Dzyabchenko, V.I. Shilnikov, I.A. Suslov, J. Structural Chem. **38**, 936 (1997).
35. W.I.F. David, R.M. Ibberson, J.C. Matthewman, K. Prassides, T.J.S. Dennis, J.P. Hare, H.W. Kroto, R. Taylor, D.R.M. Walton, Nature **353**, 147 (1991).
36. S. Okada, S. Saito, A. Oshiyama, Phys. Rev. Lett. **83**, 1986 (1999).